Transition Met Chem (2010) 35:263–270
DOI 10.1007/s11243-009-9322-9

Synthesis, characterization and catalytic properties of heterogeneous iron(III) tetradentate Schiff base complexes for the aerobic epoxidation of styrene

Ying Yang · Jingqi Guan · Pengpeng Qiu · Qiubin Kan

Received: 1 November 2009 / Accepted: 4 December 2009 / Published online: 24 December 2009

Abstract A series of hybrid mesoporous SBA-15 materials containing four iron(III) Schiff base complexes of the type $[FeL^{x}(NO_3)]$ ($x = 4$–7, L = *N*,*N*′-bis(salicylidene) ethylenediamine, *N*,*N*′-bis(salicylidene)diethylenetriamine, *N*,*N*′-bis(salicylidene)o-phenylenediamine, *N*,*N*′-bis(3-nitro-salicylidene)ethylenediamine) was synthesized by a post-grafting route. The XRD, N_2 adsorption/desorption and TEM measurements confirmed the structural integrity of the mesoporous hosts, and the spectroscopic characterization techniques (FT-IR, UV–vis spectroscopy, ^{1}H NMR) confirmed the ligands and the successful anchoring of iron(III) Schiff base complexes over the modified mesoporous support. Quantification of the supported ligand and metal was carried out by TG/DSC and ICP-AES techniques. The catalyst FeL^{7}-SBA resulting from N,N′-bis(3-nitro-salicylidene)ethylenediamine) ligand was considerably active for the aerobic epoxidation of styrene, in which the highest conversion of styrene reached 83.6%, and the selectivity to styrene oxide was 83.0%. Moreover, it was also found that the catalytic activity increases with the decrease in the electron-donating ability of the Schiff bases, and the selectivity varies according to the types of substituents in the ligands.

Introduction

Covalent immobilization of olefin epoxidation catalysts onto solid supports can increase catalyst stability and allow for product separation [1]. In this field, polystyrene (PS), zeolite-Y, M41S and mesoporous carbon-anchored Cu(II), VO(II), Mn(III), Cr(III), Bi(III), Mo(VI) and Co(II) complexes have been widely used for the oxidation of cyclohexanol [2], selective epoxidation of olefins [3–7] or decomposition of H_2O_2 [8]. The use of dioxygen or air as the oxidant for such processes is particularly attractive from both economic and environmental standpoints. However, triplet ground state of O_2 disfavors reactions with singlet organic compounds. Thus, O_2 combined with a sacrificial co-reductant, e.g., O_2–H_2 [9], O_2–Zn powder [10] and O_2-organic reductant such as alcohol or aldehyde [11] are required in the reaction mixture. Worthy of special mention is the work of Lyons and Ellis employing perhalogenated metal porphyrins as active catalysts for the oxidation of hydrocarbons by O_2 under mild conditions [12]. However, the difficulty and high cost of synthesis are problems limiting the use of perhalogenated metal porphyrins as catalysts in hydrocarbon oxidations. Therefore, we have developed a series of iron(III) tetradentate Schiff base catalysts that are more easily prepared and have features in common with metalloporphyrins with respect to their structure and catalytic activity. Bell and coworkers have systematically studied the detailed factors controlling activity and selectivity of perhalogenated metal porphyrins as active catalysts for olefin epoxidation from the structural standpoint [13]. Mohebi [14] and Mohebbi [15] also studied the catalytic properties of vanadyl tetradentate Schiff base complexes for aerobic olefin epoxidation based on ancillary ligand modification.

It is generally recognized that iron complexes are less environmentally damaging than other transition-metal complexes and such complexes have received considerable attention as catalysts [16, 17]. Iron complexes consisting of porphyrin [18], phthalocyanine [19] and quinoline [20] are involved in many oxidation reactions. However, little is known about the catalytic role of iron(III) Schiff base

Y. Yang · J. Guan · P. Qiu · Q. Kan (✉)
College of Chemistry, Jilin University, Jiefang Road 2519, 130023 Changchun, Jilin, People's Republic of China
e-mail: qkan@mail.jlu.edu.cn

complexes in aerobic olefin epoxidations. The present study seems to be the first attempt to use iron(III) tetradentate Schiff base complexes for the aerobic oxidation of styrene.

Giving the increasing interest in the structure and catalytic chemistry of supported iron complexes, here we have heterogenized a novel series of iron(III) Schiff base complexes onto a silica surface via the linker 3-aminopropyltriethyloxysilane. The catalytic properties of these hybrid materials were investigated for the epoxidation of styrene using air combined with isobutyraldehyde as the oxidant.

Experimental

The synthesis procedures for various neat or heterogeneous iron(III) complexes are depicted in Scheme 1.

Synthesis of aminofunctionalized SBA-15

The mesoporous support SBA-15 (1.0 g), prepared by a literature method [21, 22], was pre-activated by heating to 120 °C for 2 h. After cooling, the 3-aminopropyltriethoxysilane (1.6 mmol in 20 mL of dry toluene) was added under N_2 atmosphere, and the mixture was stirred at room temperature for 24 h. The resulting solid was filtered off, washed, Soxhlet-extracted with CH_2Cl_2 for 24 h and dried under vacuum. Anal. found for APS-SBA-15: C, 5.4; H, 1.4; N, 1.4%.

Synthesis of substituted salicylaldehyde

5-chloromethylsalicylaldehyde (5-CM-Sal) was synthesized from salicylaldehyde by the classical chloromethylation method. In a typical synthesis, 17.5 g (160 mmol) of salicylaldehyde was treated with 24 mL of 38% aqueous formaldehyde and 1.2 g of $ZnCl_2$ in 100 mL of conc. HCl. The mixture was stirred at room temperature under N_2 atmosphere for 24 h. The resulting white solid was filtered off and repeatedly extracted with diethyl ether. The combined organic phases were washed with saturated aqueous $NaHCO_3$ and water and then dried over $MgSO_4$. The viscous oil was obtained by distillation and then subjected to crystallization in petroleum ether. The extract furnished 5-chloromethylsalicylaldehyde as white-colored needles.

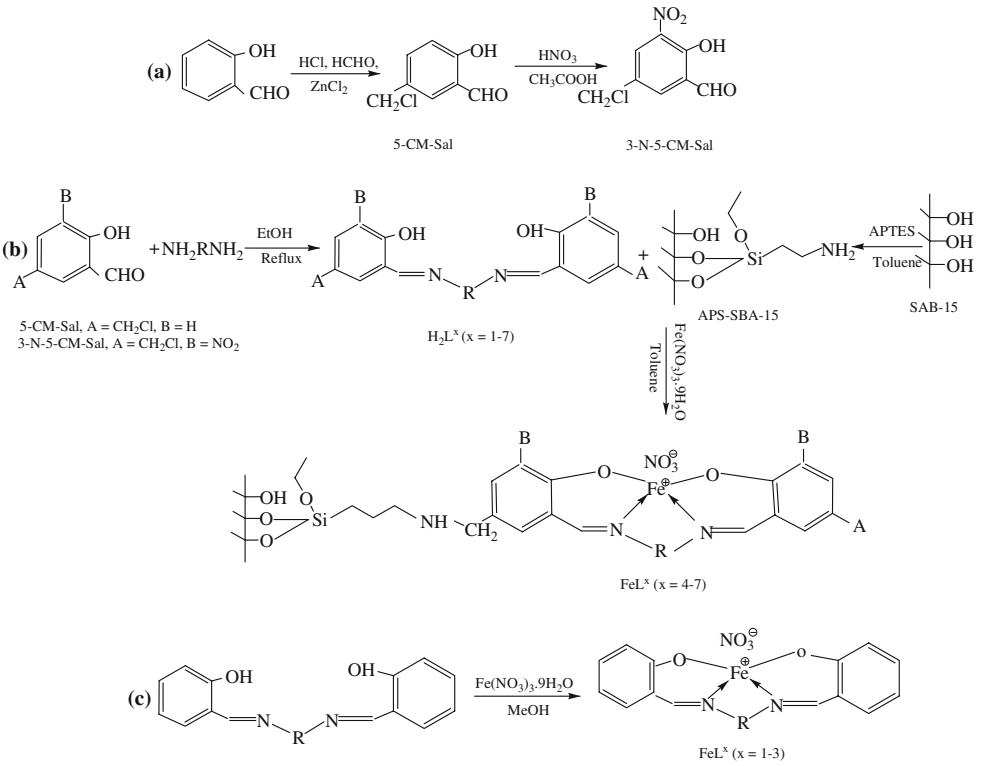

Scheme 1 Overall synthesis path for the preparation of **a** substituted salicylaldehyde, **b** SBA-15 anchored iron(III) complexes and **c** homogeneous iron(III) complexes. H_2L^x (x = 1–7): H_2L^1, R = CH_2CH_2, A = H, B = H; H_2L^2, R = $CH_2CH_2NHCH_2CH_2$, A = H, B = H; H_2L^3, R = Ph, A = H, B = H; H_2L^4, R = CH_2CH_2, A = CH_2Cl, B = H; H_2L^5, R = $CH_2CH_2NHCH_2CH_2$, A = CH_2Cl, B = H; H_2L^6, R = Ph, A = CH_2Cl, B = H; H_2L^7, R = CH_2CH_2, A = CH_2Cl, B = NO_2. FeL^x (x = 4–7): FeL^4-SBA, R = CH_2CH_2, A = CH_2Cl, B = H; FeL^5-SBA, R = $CH_2CH_2NHCH_2CH_2$, A = CH_2Cl, B = H; FeL^6-SBA, R = Ph, A = CH_2Cl, B = H; FeL^7-SBA, R = Ph, A = CH_2Cl, B = NO_2. FeL^x (x = 1–3): FeL^1, R = CH_2CH_2, A = H, B = H; FeL^2, R = $CH_2CH_2NHCH_2CH_2$, A = H, B = H; FeL^3, R = Ph, A = H, B = H

Found: C, 57.6; H, 4.1%. Anal. Calc. for $C_8H_7O_2Cl$: C, 56.3; H, 4.1%. FTIR (KBr pellets, cm^{-1}): 3240 (OH), 2925, 2873, (Aliph-H), 1659 (C=O), 1260 (CH_2Cl), 772 (C–Cl). UV–vis, λ (nm): 224, 257, 332. ^1H NMR ($CDCl_3$, TMS, δ ppm): 11.07 (1H, s, OH), 9.90 (1H, s, CHO), 7.59 (1H, s, Ar–H), 7.26–7.19 (1H, d, Ar–H), 7.02–6.08 (1H, d, Ar–H), 4.59 (1H, s, CH_2Cl).

3-nitro-5-chloromethylsalicylaldehyde (3-N-5-CM-Sal) was synthesized as follows: 0.72 mL of fuming nitric acid was added dropwise to a vigorously stirred mixture of 5-chloromethylsalicylaldehyde (2.88 g) and acetic acid (3.36 mL). After the addition was completed, the mixture was stirred at 35 °C for 3 h. The yellowish product was collected by filtration and recrystallization from benzene. Found: C, 44.3; H, 2.8; N, 6.4%. Anal. Calc. for $C_8H_6ClNO_4$: C, 44.6; H, 2.8; N, 6.5%. FTIR (KBr pellets, cm^{-1}): 3246 (OH), 2932, 2876, (Aliph-H), 1666 (C=O), 1265 (CH_2Cl), 783 (C–Cl). ^1H NMR ($CDCl_3$, TMS, δ ppm): 11.27 (1H, s, OH), 10.42 (1H, s, CHO), 7.90 (1H, s, Ar–H), 8.15 (1H, s, Ar–H), 4.60 (1H, s, CH_2Cl).

Synthesis of ligands: H_2L^x and iron(III) complexes: FeL^x-SBA ($x = 4$–7)

The modified Schiff bases were obtained by the condensation of appropriate diamine and substituted salicylaldehyde. H_2L^x ($x = 4$–6) were prepared by the treatment of a dichloromethane solution of 5-chloromethylsalicylaldehyde (20 mmol) with ethylene diamine, diethylenetriamine or o-phenylenediamine (10 mmol). H_2L^7 was obtained by the condensation of 3-nitro-5-chloromethylsalicylaldehyde and ethylene diamine in CH_2Cl_2. The mixture was stirred under N_2 atmosphere at room temperature for 24 h. The ligands were isolated by filtration, washed with CH_2Cl_2 and characterized by FT-IR, UV–vis spectroscopy and ^1H NMR (see Tables 1 and 2).

These Schiff base ligands were immobilized on mesoporous SBA-15 based on the nucleophilic reaction between the chloromethyl modified Schiff bases and the aminopropyl functionalized SBA-15. In a typical synthesis, 0.8 mmol of ligand was added to 0.5 g of APS-SBA-15 in dry toluene and stirred at reflux temperature for 24 h to obtain the hybrid materials H_2L^x-SBA ($x = 4$–7). FeL^x-SBA was obtained by stirring 0.41 g of H_2L^x-SBA with 0.11 g of $Fe(NO_3)_3{\cdot}9H_2O$ in MeOH at room temperature for 12 h. The resulting solid was filtered and Soxhlet-extracted with CH_2Cl_2 to remove untethered species and then dried in vacuum.

Table 2 IR and electronic spectral data of compounds

Compound	Selective IR bands (cm^{-1})				Transition frequency (λ_{max}/nm)
	C=N	C–O	C–Cl	Fe–O/ Fe–N	
H_2L^1	1635	1280	–	–	249, 281, 334, 401
FeL^1	1623	1298	–	539/413	233, 312, 362, 521
H_2L^2	1629	1268	–	–	240, 275, 320, 389
FeL^2	1618	1305	–	582/419	235, 321, 375, 515
H_2L^3	1610	1274	–	–	225, 267, 289, 390
FeL^3	1605	1309	–	532/454	252, 283, 356, 505
H_2L^4	1638	1290	698	–	236, 287, 380
H_2L^4-SBA	1635	1280	–	–	254, 281, 313, 378, 430
FeL^4-SBA	1629	1305	–	554	256, 280, 315, 401, 526
H_2L^5	1631	1279	766	–	241, 290, 334, 400, 421
H_2L^5-SBA	1630	1286	–	–	229, 247, 280, 313, 404
FeL^5-SBA	1628	1292	–	543	210, 259, 329, 398, 529
H_2L^6	1617	1276	751	–	250, 270, 292, 349
H_2L^6-SBA	1614	1284	–	–	247, 278, 311, 393
FeL^6-SBA	1612	1305	–	563	280, 329, 391, 565
H_2L^7	1644	1296	702	–	238, 278, 318, 360, 454
H_2L^7-SBA	1641	1285	–	–	241, 277, 316, 359, 455
FeL^7-SBA	1636	1308	–	543	234, 331, 364, 398, 522

Synthesis of ligands: H_2L^x and iron(III) complexes: FeL^x ($x = 1$–3)

Schiff base ligands H_2L^x ($x = 1$–3) and the corresponding iron(III) complexes FeL^x ($x = 1$–3) were prepared by a similar manner to that reported in the literature [23].

Table 1 ^1H NMR chemical shift (δ in ppm) of compounds H_2L^x ($x = 1$–7)

Compound[a]	O–H	CH=N	H (aromatic)	CH_2Cl	Methylene
H_2L^1	13.20 (s)	8.35 (s)	7.30–6.80 (m)	–[b]	3.91 (t)
H_2L^2	13.22 (s)	8.50 (s)	7.10–6.40 (m)	–	4.0–2.5 (m)
H_2L^3	13.08 (s)	8.52 (s)	7.80–6.80 (m)	–	–
H_2L^4	11.12 (br)	8.44, 8.40 (s)	7.83–6.98 (m)	4.44 (s)	3.19–3.10 (t)
H_2L^5	12.08 (br)	8.39, 8.34 (s)	7.99–7.00 (m)	4.43 (s)	3.40–3.20 (m)
H_2L^6	13.04 (br)	8.42 (s)	7.83–6.89 (m)	4.25 (s)	–
H_2L^7	13.40 (br)	8.65 (s)	8.03–7.12 (m)	4.56 (s)	3.45–3.6 (m)

[a] *br* broad, *s* singlet, *t* triplet and *m* multiplet

[b] Not detected

Catalytic oxidations

The epoxidation of styrene with air was carried out in a batch reactor. In a typical run, 10 mmol of styrene and 50 mg of catalyst (5 mg for the neat iron catalyst) were charged into a 100 mL two-necked flask equipped with a condenser and with an air pump. The dry air with a stable flow rate of 80 mL/min controlled by a flowmeter was bubbled into the bottom of the reactor. The liquid organic products were quantified by using a gas chromatograph (Shimadzu, GC-8A) equipped with a flame detector and an HP-5 capillary column. The liquid organic products were identified by comparison with authentic samples and GC–MS coupling.

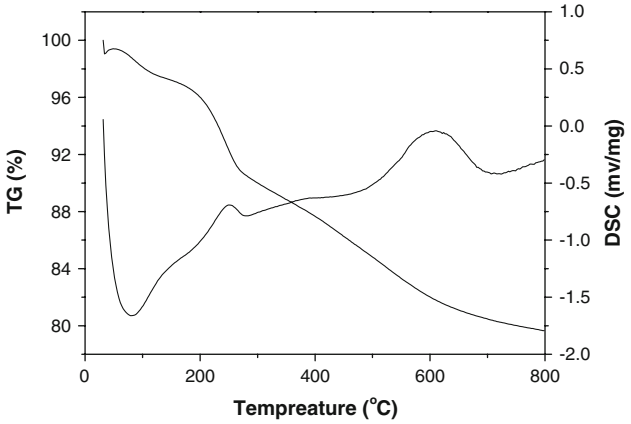

Fig. 1 TG and DSC profile of FeL^4-SBA

Results and discussion

Spectroscopic characterization

^1H NMR spectra (recorded in DMSO-d_6) of the tetradentate Schiff base ligands of N_2O_2 donor sets possess two phenolic and azomethine groups (Table 1). ^1H NMR spectra of all the Schiff bases H_2L^x show the aromatic protons as multiplet in the range 7.99–6.80 ppm and O–H protons of phenolic groups ranging from 13.20 to 10.04 ppm [14]. The azomethine protons appear at 8.44–8.34 ppm. These functional groups can also be identified by FT-IR and UV–vis spectroscopy. As illustrated in Table 2, IR bands of H_2L^x in the 1644–1610 and 1308–1268 cm^{-1} can be attributed to the C=N and C–O stretching vibrations [24]. These bands register a redshift of 3–12 cm^{-1} and a blueshift of 6–37 cm^{-1} in the iron(III) complexes, respectively. The shifts support the participation of the azomethine and phenolic oxygen of these ligands in binding to the metal ions [24]. Electronic spectra of FeL^x-SBA show bands in the visible region attributed to ligand-to-metal charge transfer (LMCT) O2p or N2p → Fe3d. The ultraviolet bands in the regions of 250–280 nm and 312–360 nm due to the intraligand IL (π–π^*) localized predominantly on the phenyl rings and on C=N fragments of the N_2O_2-ligands, respectively [25]. Expected d–d transitions of iron coordination field at 522–565 nm in combination with Fe–O vibrations at 556–584 cm^{-1} demonstrate the formation of iron complex on SBA-15 host. The similarity of the overall electronic spectral profiles for FeL^x-SAB suggests that they have similar coordination environments.

TG/DSC studies

The TG/DSC analysis result of FeL^4-SBA is depicted in Fig. 1. Quantification of weight loss at various steps is possible because of their nonoverlapping nature. Weight loss below 190 °C is due to the physically adsorbed water and solvent inside the pores. The 7.8% weight loss at 190–357 °C is mainly related to the combustion of amine. Larger loss of 8.4% in the temperature range from 357 to 714 °C is probably attributed to the decomposition of Schiff base groups [23]. The loading of Schiff base is 0.23 mmol/g based on the 8.4% of weight loss, and iron content is 0.35 mmol/g estimated by ICP-AES. The molar ratio of iron to ligand is approximately 1.5:1 and deviates from the theoretical value of 1:1, indicating that partial uncoordinated iron is captured and not released after the elution by CH_2Cl_2. The DSC curve agrees with the TG result. An intense exothermal peak at 605 °C is observed. The much higher temperature peak of FeL^4-SBA than that of H_2L^4-SBA (586 °C) gives another piece of evidence for the existence of iron complexes in the hybrid materials. TG/DSC analysis data of other supported iron complexes are listed in Table 3. It is clear that all ligand loadings are similar, which facilitates comparative study of the role of iron(III) compounds with different substituted ligands on catalytic activity.

Structural integrity studies

The powder XRD patterns for SBA-15, H_2L^4-SBA and FeL^4-SBA are depicted in Fig. 2. Three reflections, one strong peak at (100) and two with low intensity at (110) and (200) planes, are seen in the range $2\theta = 0.8$–$2°$ for the mesoporous SBA-15 material, indicating a significant degree of long-range ordering and well-formed hexagonal pore arrays [26]. For the hybrid materials, the relative intensities of the prominent diffraction peak (100) decreased after the introduction of bulky organometallic groups. The intensity reduction may be mainly due to contrast matching between the silicate framework and organic moieties that are located inside the channels of SBA-15 [27]. TEM images provide a direct visualization of well-ordered hexagonal arrays of 1D mesoporous channels

Table 3 TG/DSC analysis data of samples

Materials	Temperature range (°C)	Weight loss (%)	Peak (°C)	Type of loss	Ligand loading (mmol/g)
H_2L^4-SBA	26–250	8	68	Endothermic	–
	250–386	8	270	Endothermic	–
	450–707	7.3	586	Exothermic	0.21
FeL^4-SBA	33–192	2.7	79	Endothermic	–
	192–357	7.8	250	Exothermic	–
	357–714	8.4	605	Exothermic	0.23
FeL^5-SBA	27–260	3.6	80	Endothermic	–
	260–310	6.7	265	Exothermic	–
	310–740	7.1	625	Exothermic	0.25
FeL^6-SBA	36–180	3.4	80	Endothermic	–
	180–314	6	267	Exothermic	–
	314–750	10	646	Exothermic	0.24
FeL^7-SBA	35–200	2.3	82	Endothermic	–
	200–324	9.2	282	Exothermic	–
	324–720	5.9	650	Exothermic	0.22

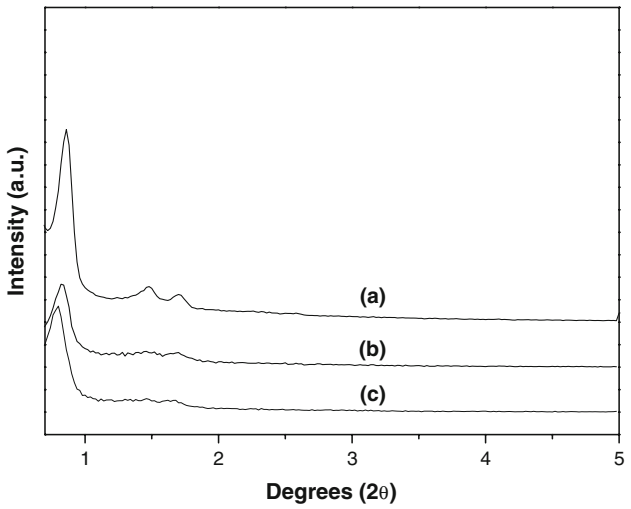

Fig. 2 XRD patterns of *a* SBA-15, *b* H_2L^4-SBA and *c* FeL^4-SBA

particularly along the direction of the pore axis or in the direction perpendicular to the pore axis (Fig. 3). The N_2 adsorption/desorption isotherms of SBA-15 and the hybrid materials are shown in Fig. 4. Obviously, the hybrid materials maintain the characteristics of type IV isotherms and show a uniform pore size distribution in the mesoporous region. However, compared to SBA-15, the ligand and complex supported samples exhibit a drastic decrease in N_2 uptake due to the relatively high loading with the comparatively bulky organometallic compounds on the surface of the mesoporous channels. The textural properties are listed in Table 4. Obviously, the hybrid materials display reduced specific surface areas, pore sizes and pore volumes, which indirectly evidences that the ligands or organometallic complexes are in the empty voids of the hexagonal channels, and thus results in increased wall thickness. A similar trend has also been observed previously [28]. Compared to H_2L^x-SBA ($x = 4, 5$), however, FeL^x-SBA ($x = 4, 5$) exhibited larger textural parameters, which is consistent with the idea reported in literature [29].

Aerobic epoxidation of styrene

Electronic effect and catalytic properties

To quantify the influence of electronic properties of iron(III) Schiff base complexes on the aerobic epoxidation of styrene, iron complexes with electron-donating and electron-withdrawing groups have been evaluated. From the data present in Table 5, FeL^4-SBA shows the highest activity with 80.9% conversion of styrene after 8 h (TOF 57.8 h^{-1}) among the three catalysts FeL^x-SBA ($x = 4$–6). A definite trend to higher activity is displayed by diimine bridge substituents on the Schiff base skeleton in the order: $FeL^4 > FeL^5 > FeL^6$. From the mechanistic point of view, the o-phenylenediimine bridge is the strongest electron-donor among three diimines, which stabilizes the positive iron(IV)-oxo species and decreases the electrophilic attack to styrene. The introduction of nitro groups into the Schiff base ligand leads to the much higher conversion of 83.6%. Similarly, the electron-withdrawing substituents are expected to destabilize the metal-oxo intermediate, making it more reactive (Scheme 2).

It is clear that the activity decreases accompanied by the elevation of iron loading for FeL^x-SBA ($x = 4$–6), which suggests that the efficiency of catalysts is strongly dependent on the electronic properties of the Schiff bases. However, are more iron species attributed to the higher activity for FeL^7-SBA? To probe this question, what is the truly active

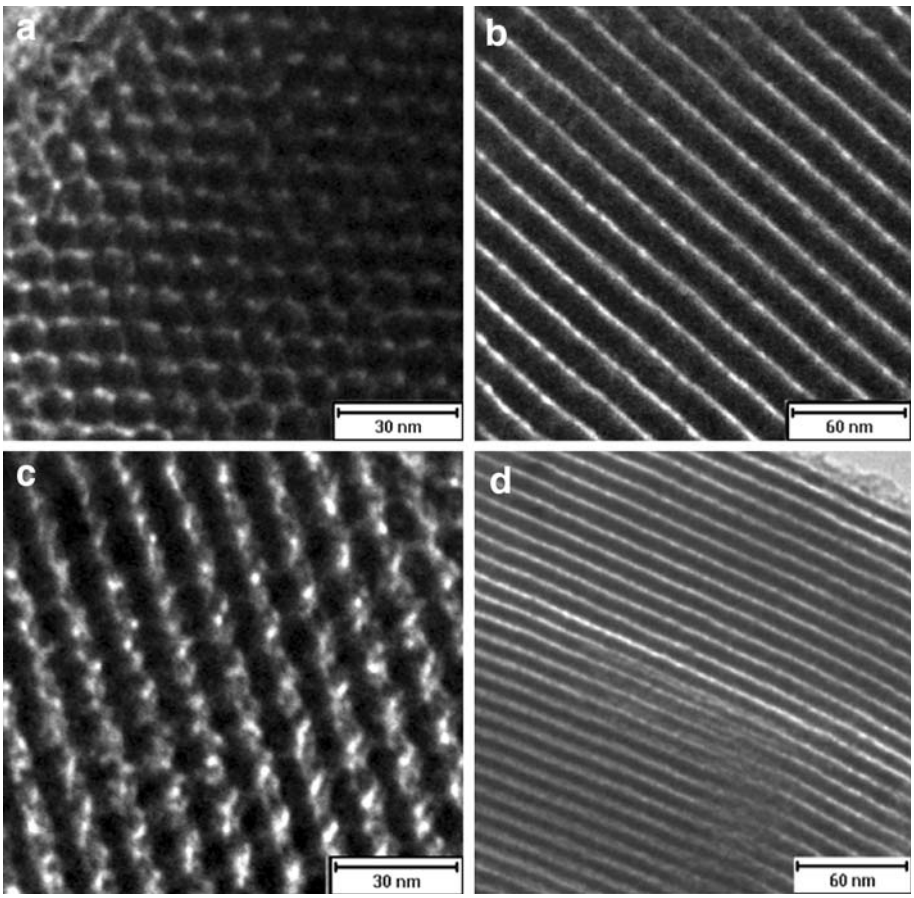

Fig. 3 TEM images of H_2L^4-SBA (**a**, **b**) and FeL^4-SBA (**c**, **d**): **a** and **c** are in the direction of the pore axis, **b** and **d** are perpendicular to the pore axis

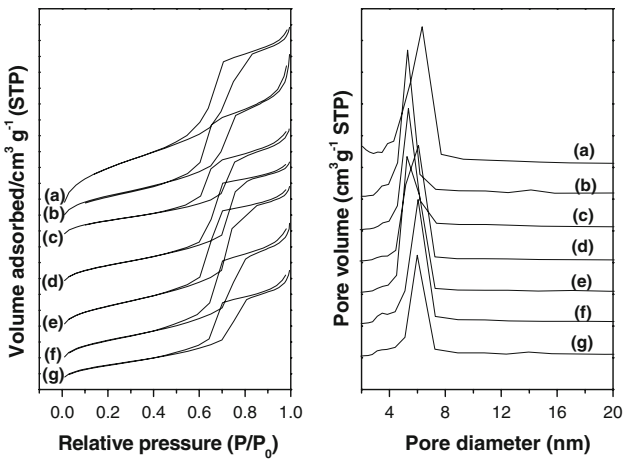

Fig. 4 N_2 adsorption/desorption isotherms and pore size distribution profiles of *a* SBA-15, *b* H_2L^4-SBA, *c* FeL^4-SBA, *d* H_2L^5-SBA, *e* FeL^5-SBA, *f* H_2L^6-SBA and *g* FeL^6-SBA

species seems crucial. Blank reaction performed over SBA-15 or H_2L^4-SBA under identical conditions shows only negligible conversion. As well as coordination to a chelate ligand, the iron(III) may also interact with the surface Si–OH. Thus, the materials of blank SBA-15 that adsorbed iron(III) were also investigated for epoxidation experiment. It turned out that the conversion of styrene was almost 0% after 8 h. By contrast, the corresponding neat iron complexes are highly active and display slightly lower selectivity to styrene oxide than the corresponding heterogeneous catalysts FeL^x-SBA. These observations suggest that the oxidations occur due to the catalytic nature of the anchored iron(III) Schiff base complexes. It is reasonable to speculate that the catalytic activity is related to ligand loading since overall ligands are binding to iron(III). Therefore, the catalytic activity of FeL^x-SBA with similar ligand loading is mainly determined by electro-withdrawing effect of substituted ligands. That is why FeL^7-SBA is the most active catalyst with 83.6% conversion of styrene and with a lower TOF value (38.1 h^{-1}).

Possible mechanism for the aerobic epoxidation of styrene

The catalytic properties and electronic effects discussed above are closely correlated with the mechanism. Two major pathways involving either a high valent metal-peroxo/oxo species or free radical intermediates have been proposed for the oxidation of styrene by O_2 [30–32]. The mechanistic model of Figueiredo [33], Ramaraj [34] and Ghandi [35] can

Table 4 Analysis results of textural characteristics

Materials	S_{BET} ($m^2\ g^{-1}$)	V_p ($cm^3\ g^{-1}$)	D_p^a (nm)	D_{100}^b(nm)	A_o (nm)	Wall thickness[c] (nm)
SBA-15	892	1.01	6.35	10.28	11.87	5.52
H_2L^4-SBA	409	0.72	5.31	10.71	12.37	7.06
FeL^4-SBA	302	0.53	5.34	11.19	12.92	7.58
H_2L^5-SBA	340	0.61	6.11	10.50	12.12	6.01
FeL^5-SBA	416	0.71	5.25	11.09	12.80	7.55
H_2L^6-SBA	387	0.66	6.03	11.10	12.82	6.79
FeL^6-SBA	285	0.52	6.01	11.43	13.20	7.19

[a] Obtained from the desorption branch

[b] Calculated from XRD results

[c] $\text{Wall thickness} = A_o - D_p\left(A_o = 2D_{100}/\sqrt{3}\right)$

Table 5 Catalytic results of homogeneous and heterogeneous iron(III) complexes in aerobic epoxidation of styrene

Catalysts	Metal loading (mmol/g)	Styrene conversion (%)[a]	TOF (h^{-1})[c]	Product selectivity (mol%)[d]		
				So	Bza	Others
FeL^4-SBA	0.35 (1.9)[b]	80.9	57.8	59.7	32.8	7.5
FeL^5-SBA	0.43 (2.4)	70.2	40.8	53.5	40.5	6.0
FeL^6-SBA	0.49 (2.7)	48.2	24.6	51.4	44.6	4.0
FeL^7-SBA	0.55 (3.1)	83.6	38.1	83.0	8.9	8.1
FeL^1	3.10 (17.3)	83.1	66.9	51.2	44.1	4.7
FeL^2	2.97 (16.5)	86.2	72.6	43.2	55.0	1.8
FeL^3	2.70 (15.1)	77.4	71.6	46.8	50.6	2.6

[a] Reaction conditions: catalyst 50 mg for FeL^x-SBA ($x = 4$–7), 5 mg for FeL^x ($x = 1$–3), styrene 1.14 mL (10 mmol), CH_3CN 10 mL, flow of air 80 mL/min, isobutyraldehyde 2.28 mL (25 mmol), temperature 80 °C and duration 8 h

[b] wt.%

[c] TOF, h^{-1}: (turnover frequency) moles of substrate converted per mole metal ion per hour

[d] So: Styrene oxide, Bza: benzaldehyde and Others: including benzoic acid, phenylacetaldehyde and 1-phenyl-ethane-1,2-diol

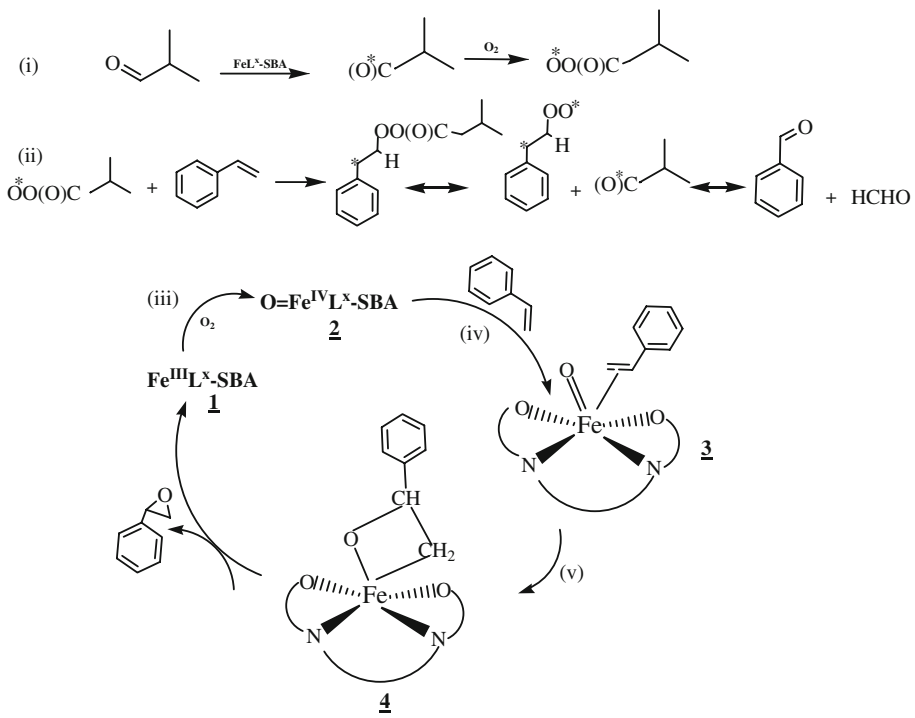

Scheme 2 Proposed mechanism for aerobic epoxidation of styrene with iron(III) complexes in the presence of isobutyraldehyde

be extended for our system. The proposed mechanism for the aerobic epoxidation of styrene is described in Scheme 2. (1) Isopropylacyl radical produced through the electron transfer to iron(III) affords the corresponding peroxide radical in reaction with O_2. (2) A radical chain reaction leads to benzaldehyde. (3) The oxo-complex $[O=Fe^{IV}(\text{Schiff base})]^+$ generated from an iron(III) complex leads to species **2**. (4) Species **2** reacts with a molecule of styrene to give an organometallic intermediate **3**. It is followed by [2 + 2] cycloaddition of C=C to the oxo-iron bond that gives intermediate **4**. Metal-oxetane type intermediate formation is frequently invoked for explaining epoxide formation catalyzed by metal-oxo-complex [36]. This decomposes to **1** and styrene oxide. The favorable effect of electron-withdrawing groups on the selectivity to styrene oxide found in our study can be attributed to the intermediate metal-peroxo complex **4** for oxygen atom transfer to the olefin. Styrene can hardly coordinate to the iron centre when strong electron-donors are present. Thus, the radical mechanism (path ii) leads to more benzaldehyde.

Conclusions

We have succeeded in designing an active family of heterogeneous iron(III) catalysts containing inexpensive Schiff bases for styrene epoxidation by air under mild conditions. Systematic ancillary ligand substitutions demonstrate that increasing the electron-withdrawing ability of the Schiff bases promotes reaction activity and the selectivity to styrene oxide. The correlation between electronic effect and activity seems to be subjected to subtle structural effects that are not apparent in other heterogeneous systems. It may in fact offer additional possibilities for controlling reactivity through structural adjustment.

Acknowledgments Financial assistance from the National Basic Research Program of China (2004CB217804) and the National Natural Science Foundation of China (20673046) is gratefully acknowledged. We also greatly appreciate the suggestions from editor and referees concerning the improvement of this paper.

References

1. De Vos DE, Dams M, Sels BF, Jacobs PA (2002) Chem Rev 102:3615
2. Ratnasamy C, Murugkar A, Padhye S, Pardhy SA (1996) Indian J Chem 35A:1
3. Bowers C, Dutta PK (1990) J Catal 122:271
4. Knops-Gerrits P-P, Vos DD, Thibaut-Starzk F, Jacobs PA (1994) Nature 369:543
5. Agrawal DD, Bhatnagar RP, Jain R, Srivastava S (1990) J Chem Soc Perkin Trans 2:989
6. Sabater MJ, Corma A, Domenech A, Fornés V, Garcia H (1997) Chem Commun 1997:1285
7. Koner S (1998) Chem Commun 998:593
8. Jacob CR, Varkey SP, Ratnasamy P (1998) Micropor Mesopor Mater 22:465
9. Sinha AK, Seelan S, Tsubota S, Haruta M (2004) Angew Chem Int Ed 43:1546
10. Yamanaka I, Nakagaki K, Otsuka K (1995) J Chem Soc Chem Commun 11:1185
11. Meunier B (1992) Chem Rev 92:1411
12. Lyons JE, Ellis PE (1991) Catal Lett 8:45
13. Stephenson NA, Bell AT (2007) J Mol Catal A Chem 272:108
14. Boghaei DM, Mohebi S (2002) J Mol Catal A Chem 179:41
15. Mobebbi S, Sarvestani AI (2006) Transition Met Chem 31:749
16. Lu XH, Xia QH, Zhan HJ, Yuan HX, Ye CP, Su KX, Xu G (2006) J Mol Catal A Chem 250:62
17. Xia QH, Ge HQ, Ye CP, Liu ZM, Su KX (2005) Chem Rev 105:1603
18. Nur H, Hamid H, Endud S, Hamdan H, Ramli Z (2006) Mater Chem Phys 96:337
19. De Vos DE, Jacobs PA (2000) Catal Today 57:105
20. Liu CB, Shan YK, Yang XG, Ye XK, Wu Y (1997) J Catal 168:35
21. Zhao DY, Feng JL, Huo QS, Melosh N, Fredrickson GH, Chmelka BF, Stucky GD (1998) Science 279:548
22. Mckittrick MW, Jones CW (2003) Chem Mater 15:1132
23. Jin C, Fan WB, Jia YJ, Fan BB, Ma JH, Li RF (2006) J Mol Catal A Chem 249:23
24. Kilic A, Tas E, Deveci B, Yilmaz I (2007) Polyhedron 26:4009
25. Soundiressane T, Selvakumar S, Ménage S, Hamelin O, Fontecave M, Singh AP (2007) J Mol Catal A Chem 270:132
26. Raj NKK, Deshpande SS, Ingle RH, Raja T, Manikandan P (2004) Catal Lett 98:217
27. Jia MJ, Seifert A, Thiel WR (2003) Chem Mater 15:2174
28. Joseph T, Hartmann M, Ernst S, Halligudi SB (2004) J Mol Catal A Chem 207:131
29. Kruk M, Celer EB, Jaroniec M (2004) Chem Mater 16:698
30. Sheldon RA (1993) Topics Curr Chem 23:164
31. Kim J, Harison RG, Kim C, Que L Jr (1996) J Am Chem Soc 118:4373
32. Macfaul PA, Arends IWCE, Ingold KU, Wayner DDM (1997) J Chem Soc. Perkin Trans 2:135
33. Silva M, Freire C, De Castro B, Figueiredo JL (2006) J Mol Catal A Chem 258:327
34. Sivasubramanian VK, Ganesan M, Rajagopal S, Ramaraj R (2002) J Org Chem 67:1506
35. Farzaneh F, Tayebi L, Ghandi M (2007) React Kinet Catal Lett 91:333
36. Jorgensen KA (1989) Chem Rev 89:431